

## Article

# Demand Response with Electrical Heating in Detached Houses in Finland and Comparison with BESS for Increasing PV Self-Consumption

Juha Koskela \*  and Pertti Järventausta

Unit of Electrical Engineering, Tampere University, Korkeakoulunkatu 7, FI-33720 Tampere, Finland

\* Correspondence: juha.j.koskela@tuni.fi

**Abstract:** Distributed electric power production by small-scale customers is increasing continuously. Photovoltaic production is a popular method of producing self-energy for customers. Additionally, power systems require more flexibility when weather-dependent renewable energy production increases. Small-scale customers can increase the self-consumption of self-produced energy by using batteries or a demand response operation. However, batteries require high investment, and demand response operations induce a loss of comfort. Customers who heat their buildings using electric heaters are a good target for demand response operations because their heating can be controlled with limited changes in the indoor temperature. The demand response potential of a building can be defined by simply using customer load profiles and knowledge of the outdoor temperature. Any other information is not required in the proposed novel method. A tolerable variation in indoor temperature corresponds to considerably smaller battery capacity, though it is still a significant amount. With an optimally sized photovoltaic system, it is possible to use both methods simultaneously to increase self-consumption. Maximal benefits can be attained from both methods if the battery system is used as a primary control and the demand response is used as a secondary control. The defined novel method for determining the demand response potential of small-scale customers can also be used when estimating the flexibility of a large customer group. Small-scale customers together can provide significant flexible capacity when their electrical heating is centrally controlled.

**Keywords:** demand response; battery; buildings; photovoltaic



**Citation:** Koskela, J.; Järventausta, P. Demand Response with Electrical Heating in Detached Houses in Finland and Comparison with BESS for Increasing PV Self-Consumption. *Energies* **2023**, *16*, 497. <https://doi.org/10.3390/en16010497>

Academic Editor: Alessandro Cannavale

Received: 25 November 2022

Revised: 23 December 2022

Accepted: 29 December 2022

Published: 2 January 2023



**Copyright:** © 2023 by the authors. Licensee MDPI, Basel, Switzerland. This article is an open access article distributed under the terms and conditions of the Creative Commons Attribution (CC BY) license (<https://creativecommons.org/licenses/by/4.0/>).

## 1. Introduction

Flexibility will have a key role in future power systems as electrification and 100% renewable energy production are being pursued [1]. In power systems, flexibility can be implemented through many applications and at various scales. One method is to use demand response (DR) operations in which the consumption flexes when production changes. Flexible loads can be of various sizes, and a large number of small loads can form a larger group of flexible loads. Flexible loads can be controlled for the direct benefit of customers using their own control system, or they can be centrally controlled to benefit the system such that all customers benefit [2]. A customer self-control system can be called a price-based DR program, in which customers make load changes by responding to economic signals. A centrally controlled system can be called an incentive-based DR program, in which customers are offered payments for reducing their specific loads over a given period. The grid contains many detached houses, which are considerably small loads from the power system perspective but together create a significant flexible load. This paper focuses on DR with electric heaters in a Nordic area where there are a lot of electrically heated detached houses. A high number of small-scale customers from Finland were studied.

In the future, small-scale energy production will increase when it becomes economically more attractive to domestic customers [3]. Household-level customers typically use a

small photovoltaic (PV) system; thus, the production is mostly used in self-consumption, because the economic value of the produced energy for self-consumption is significantly higher than the value of produced energy for selling to the market [4]. Flexibility, for example through the use of battery systems, enables fixed-sized PV panels to better react and adjust to self-consumption increases [5]. Historically, power transfer in the power lines is conveyed from power plants to customers. Multiple small-scale power plants (e.g., household small-scale PV systems) around the grid can reform the grid and energy flows bidirectionally. Increasing weather-dependent energy production and distributed energy resources (DER) set new requirements for power systems [1]. The grid must be redesigned toward bidirectional function, and the power system requires more flexibility for efficient operation in the future. High flexibility will decrease the negative effects of increasing DER, e.g., the requirement to reinforce the grid. Child et al. demonstrated that customers who have PV production systems with battery storage can reduce the requirement for transmission interconnections by 6% [1].

The benefits of using flexibility to increase self-consumption have been examined in many papers. Merei et al. presented a techno-economic analysis of a PV–battery system, and the results indicated that increasing self-consumption through the use of batteries has cost problems associated because of high battery investment costs [6]. The results of Ref. [7] show that low discount rates and debt financing may significantly increase the profitability of battery investment. The potential of battery use with PV systems also increases if the lifetime of the battery increases. Angenendt et al. presented a forecast-based operation strategy for this [8]. Puranen et al. focused on a case study from Finland for a techno-economic analysis of energy storage concepts with residential PV systems [9]. The profitability of battery systems with PV production under different retail tariffs was studied in Ref. [10]. A comparative study of different control strategies for PV–battery systems is presented in Ref. [11] for an office building environment.

DR operations are effective for increasing distributed PV penetration [12]. The effectiveness of DR operations depends on the operation algorithms, and Sivaneasan et al. [13] presented one option for using such algorithms. Nyholm et al. [14] presented an economic assessment of PV production in Sweden with a special focus on the impacts of DR. Additionally, in many papers, batteries and DR have been combined [15,16].

However, earlier studies did not publish a wide comparison of battery storage and heating power DR with long-period simulations and did not explore the effects the battery and DR operation have on each other. In this novel research, we studied the possibility of using batteries and DR in parallel and the potential of using both. Earlier studies, such as the study conducted by Lorenzi et al., compared battery storage and water boiler DR from an economic perspective, and the results demonstrated the high potential of DR operations compared to batteries [17].

Heating power DR has rarely been studied even though it has high potential. One reason for this is that every building is different, and the features of buildings are difficult to approximate. Generally, studies require a building model that considers the insulation and ventilation of the building. Bashir et al. formed a building model based on Finnish construction requirements, and it was used to evaluate the storing of PV production as heat for the building [18]. This method aids in evaluating the possible power of DR operations and the changes in indoor temperature that occur in a building during operation. This paper presents a novel method of evaluating the DR potentials of buildings from electricity load profiles without any other knowledge of the building. In previous studies, values from typical buildings and calculations based on theoretical features were used, though real building data were used in Ref. [19]. For evaluating the DR potential of space heating, Nyholm et al. used constant effective heat capacity, which was taken from previous studies [20]. The model presented in this paper calculates accurate thermal storage features for every customer. Additionally, as an improvement on previous studies, the number of customers in the study group was large and the study period was long. For example, while this paper uses a year-long study period, Zhang and Guéquen used a 24 h period [21].

In earlier papers, the number of studied buildings was low and buildings features were usually from some form of test house [22] or were based on the average features used in the studied area [23].

Naturally, the potential of DR is limited and depends on the customers' load profile. Possible DR devices should be high-load devices whose time of use can be flexible. Electrical heating is appropriate for DR because houses include thermal storage capacities. Short breaks in heating do not dramatically decrease the indoor temperature, and in controlled systems, breaks can be prepared by overheating the house before the breaks. If heating is used for DR, the DR capacity depends on the outdoor temperature and limits set for indoor temperature. DR should cause only a minimal loss of comfort for the customer, but it always causes some effects. With the use of a battery, a customer's load profile can be modified without any loss of comfort. The capacity of the battery and charging and discharging power are the only limits of its use. Even if the DR and battery are used for the same purpose, their basic principles in how benefits are formed are different. Therefore, comparison between DR and batteries is very difficult.

Indoor temperature limits varied significantly in earlier research [24]. Many people do not notice an indoor temperature change of  $\pm 0.5$  °C over the course of an hour, but a  $\pm 2$  °C change can affect the comfort of most people [25]. Additionally, the law sets limits. In Finland, the terms of electricity supply define that an electrical heater can be switched off for a maximum of 1.5 h when continuously controlled by an aggregator, and the total switch-off time should be 5 h in a day [26]. This paper compares the use of DR and a battery by comparing 1 and 2 °C flexibility in indoor temperature to the corresponding size of the battery. This novel information provides knowledge about the possibilities of DR and battery use. The most significant problem relating to battery use has often been high investment costs and how those costs compare to the potential benefits. The comparison method used in this paper is very extensive because it enables systems to be compared even if the investment costs or electricity prices change over time.

The objective of the developed novel method for evaluating the flexibility of building heating is to determine a simple method of comparing heating demand usage for DR with a battery. Additionally, the method provides the possibility of evaluating DR potential in larger groups. The results of this study can be utilized in many applications. Small-scale customers can use the results when making future investment decisions on whether it is better to invest in a DR control system or energy storage system and whether there may be problems if both are used. Service providers can develop their products to sell to customers. Additionally, aggregators who sell incentive-based DR programs to customers can estimate potential DR capacity. The method also provides the possibility of estimating the DR potential of all local electric heating customers within the grid.

For small-scale customers, the possibility of storing surplus PV energy is most important; therefore, the research focus was on this control target. The same flexible capacity can be used for other control targets, e.g., market price-based control or decreasing maximum power with power-based distribution tariffs. The results of this paper can be used to estimate the potential of decreasing the maximum power. Market price-based control is a potential topic for future research because its economic potential is currently very low, particularly with a battery system [27].

Storing surplus PV energy in a building's heat means that the indoor temperature increases temporarily. The thermal features of buildings operate similarly in both directions; therefore, DR operation can be upshifting (e.g., surplus PV energy storing) or downshifting (e.g., decrease in maximum power). Downshifting operations can be effective in scenarios in which consumption is very high owing to very cold outdoor temperatures, and also when maximum power should be limited to avoid local grid reinforcements. This paper also investigates the DR potential of a large local customer group.

This study utilizes simulations. New load profiles for customers were modeled in a simulator and PV production and flexibility options added. Simulations are a good way to study phenomena involving a large number of customers with minimal time and

cost. Self-coded simulators provide the possibility of studying novel methods of evaluating DR potential with the minimum amount of information from customers. Modeling simulators for commercial buildings need much more specific information in terms of buildings features.

The remainder of this paper is divided into six sections. Section 2 presents the theoretical background of simulation models and calculations. Section 3 includes the initial input data and introduces the study on customers' DR capacity, and examples are presented for how the coefficients are solved and their effect on DR capacity. Section 4 presents the results of simulations and a comparison between a DR operation and battery system in regard to storing surplus PV energy. Section 5 presents the results of a DR capacity study with a large local customer group. A discussion is presented in Section 6, and the conclusions of the paper are shared in Section 7.

## 2. Components of the Simulation Model

### 2.1. Small-Scale Electrical Energy Self-Production with Solar Panels

In the simulations in this study, we assumed that detached house customers had small-scale PV energy production systems. PV production depends on geographical location, weather conditions, and time of day and year. Owing to many variables, the momentary power of PV production varies significantly. In this study, PV production was modeled with a mathematical model for the same area in which the studied detached house customers were located and included realistic weather data. A similar PV model was presented earlier in Ref. [4].

#### 2.1.1. Solar Irradiance Model for Tilted Panels

The model of PV production is based on the solar irradiance of a tilted panel in a known location on Earth. Global solar irradiance can be mathematically modeled and it can be divided into three components: the direct beam ( $G_{b,i}$ ), the diffuse component ( $G_{d,i}$ ), and the reflected component ( $G_{r,i}$ ) [28]. Global irradiance is the sum of the irradiance components, i.e.,  $G_i = G_{b,i} + G_{d,i} + G_{r,i}$ . In this paper, the azimuth angle of modeled solar panels is assumed to be  $0^\circ$ , i.e., panels are tilted straight to the south and the angle of inclination  $\beta$  is  $45^\circ$ . Beam irradiance can be modeled accurately if the conditions of the sun are assumed to be constant, and it can be calculated using  $G_{b,i} = G_b (\cos \theta_i / \sin \alpha_s)$ , where  $G_b$  is horizontal beam irradiance,  $\theta_i$  is the angle of incidence onto the surface based on the azimuth angle of the sun, and  $\alpha_s$  is solar elevation [29]. Diffuse irradiance on a tilted surface can be calculated using  $G_{d,i} = G_d (1 + \cos \beta)/2$ , where  $G_d$  is the horizontal diffuse irradiance. The reflected irradiance can be calculated using  $G_{r,i} = \rho_g G (1 - \cos \beta)/2$ , where  $\rho_g$  is the average reflectance of the reflecting surface and  $G$  is horizontal global irradiance, which is used because both the beam and diffuse irradiance are assumed to reflect isotropically.

Different irradiance components are modeled with mathematical methods and several competing decent models are available. The Perez All-Weather Sky model was observed to be the overall best model for modeling diffuse irradiance involving Finnish conditions; however, when solar panels were tilted to the south, the Reindl model was better [29]. The Reindl model was used in this paper. The Perez model is introduced in [30] and the Reindl model in [31]. Additionally, in Ref. [32], the Reindl model is considered one of the best diffuse solar irradiance models. The brightening factor ( $k_T$ ) models the cloudiness of the sky, and in the Reindl model, it is modeled using the ratio of horizontal diffuse irradiance to horizontal global irradiance. In this paper, a brightening factor based on cloudiness probability in Finland was used [33].

Reflectance values are used to model reflecting irradiance. Average reflectance has two constant values in year-long simulations. During the winter season (December–April), the average reflectance is set to  $\rho_g = 0.58$ , which corresponds to the reflectance of snow, because snow is typically on the ground during this period in Finland. At other times of the year, it is set to  $\rho_g = 0.24$ , which corresponds to the reflectance of dark roofing materials and deciduous trees, which are the materials assumed to be directly adjacent to the solar panels.



### 2.1.2. PV Production Model

The power of PV production ( $P_{PV}$ ) can be calculated using Equation (1), where  $P_{STC}$  is the nominal power in standard test conditions (STC),  $\beta_P$  is the solar cell power temperature coefficient (0.006),  $T_c$  is solar cell temperature, and  $T_{STC}$  is the standard solar cell test temperature (25 °C) [29]. Different types of solar panels provide slightly different power with the same solar irradiation; therefore, the verification coefficient ( $C_v$ ) is included in the equation.

$$P_{PV} = C_v P_{STC} G_i (1 - \beta_P (T_c - T_{STC})). \quad (1)$$

This PV production simulation model was used previously in [27], where it was verified by comparing model values to actual values obtained from polycrystalline silicon PV cells. Modeled PV power was systematically slightly higher than measured power; therefore,  $C_v$  is set to 0.85.

### 2.1.3. Economic Benefits of PV Production

In Finland, the price of electricity includes the price of electrical energy, the cost of distribution, and taxes. When a prosumer sells electricity to the grid, the total price of selling electricity ( $C_{s,t}$ ) is based only on the price of electrical energy. Frequently, the selling price of an energy retailer is slightly lower than the purchase price because the margin of the energy retailer is included in the purchase price, and it is thus removed from the selling price. The total purchase price of electricity ( $C_{p,t}$ ) includes the selling price of the energy retailer, distribution fees, and taxes. The main benefits of PV self-consumption result from differences in the selling and purchase prices, because the selling price is significantly lower than the price that would be paid for electricity if the self-consumed electricity ( $E_{PV,sc}$ ) were to be purchased from the grid. The economic benefits of PV production ( $EB_{PV}$ ) can be formed using Equation (2), where  $E_{PV,fg}$  is the PV production fed to the grid:

$$EB_{PV} = C_{p,t} E_{PV,sc} + C_{s,t} E_{PV,fg}. \quad (2)$$

The aim of using flexibility to increase self-consumption is to enhance the economic benefits of PV production. The sum of PV production ( $E_{PV,sc} + E_{PV,fg}$ ) remains the same, but moving the maximal amount of grid feeding ( $E_{PV,fg}$ ) toward self-consumption ( $E_{PV,sc}$ ) increases total benefits. The economic benefits depend strongly on electricity prices and pricing structures. These benefits are not calculated in this paper, but Equation (2) explains the motivation to increase self-consumption.

## 2.2. Energy Storage

A battery energy storage system (BESS) is a suitable energy storage solution for residential buildings. A BESS is the most flexible method of shifting loads because it can be controlled without depending on any other variable. Only the features and size of the battery affect charging and discharging power and the amount of energy. A high investment cost and poor profitability are the main problems that have hindered the implementation of residential BESSs [27]. The price of lithium-ion (Li-ion) batteries has decreased rapidly, and this trend is expected to continue [34]. The trend of increasing variability in electricity prices will increase the profitability of BESSs in the future [27]. Because the prices of batteries are still high, the other method of shifting loads (DR) will be a good option, whether used alone or with a BESS.

### 2.2.1. Battery Model

The modeled battery is a Li-ion battery with a lithium iron phosphate (LFP, LiFePO<sub>4</sub>) positive electrode and a graphite negative electrode. This type of battery is excellent for domestic use because of its good safety features, and it has a long cycle and calendar lifetime [35]. The BESS includes a control system, which is implemented via an inverter that requires information from all other components of the system. The battery converter includes a charge controller.

The state of charge (SOC) of the BESS is modeled in Equation (3):

$$SOC_t = 100 \frac{E_t}{E_{max}} = 100 \frac{B_{eff} B_t}{E_{max}} + SOC_{t-1}, \quad (3)$$

where  $E_t$  is the amount of stored energy at time  $t$  and  $E_{max}$  is the maximum capacity of the BESS. The variable  $SOC_t$  is the SOC at time  $t$ , and  $SOC_{t-1}$  is the SOC for the previous time step. Additionally,  $B_t$  is the energy transfer to or from energy storage, and  $B_{eff}$  is the efficiency of the transfer.

The modeling of BESS losses is a very important aspect in simulations. The efficiency of components affects the losses of the BESS. In this study, the efficiency of the inverter ( $\eta_{inv}$ ) was 98%, and DC converter efficiency ( $\eta_{dc}$ ) was 99%. The losses of the BESS primarily occur in the converters and the chemical reactions of the battery [35]. In this study, the SOC limits of the battery were set at 25%–95%, because losses increase when the SOC is near extreme values [36]. The behavior of battery losses is nearly linear with a limited charge range; therefore, in battery loss modeling, the losses can be assumed to linearly depend on the charging current ( $I_c$ ), assuming that the internal serial resistance ( $R_b$ ) is constant [36]. In this case, charging efficiency ( $\eta_c$ ) can be calculated using Equation (4):

$$\eta_c = 100 \frac{V_b - I_c R_b}{V_b}, \quad (4)$$

where  $V_b$  is the nominal voltage of the battery. The efficiency  $B_{eff}$  in (3) can be obtained by multiplying the efficiencies  $\eta_{dc}$ ,  $\eta_{inv}$ , and  $\eta_c$ . The energy transfer to or from storage ( $B_t$ ) is calculated by multiplying the charging current ( $I_c$ ) by the charging voltage ( $V_c$ ), which can be calculated using Equation (5):

$$V_c = V_b - I_c \cdot R_b \quad (5)$$

The battery used in the simulations consisted of cells. A suitable battery capacity and voltage level can be attained by connecting cells in series or parallel. The values used in the simulations of this study were an internal serial resistance of 0.026  $\Omega$ , a cell voltage of 3.3 V, and capacity for one cell of 2.5 Ah [37]. The C-rate of a battery describes the ratio of maximum power to capacity. The C-rate in this study was 0.7 C. The effect of the BESS and PV production on the customer's electricity load was modeled using equations from the grid perspective. The energy transition between the grid and customer ( $G$ ) was determined using a model based on the energy transfer to and from the BESS, the building's demand ( $D$ ), and the amount of self-produced PV energy ( $P_{dc}$ ). When the battery was charged, the energy transfer between the customer and the grid could be represented using Equation (6):

$$G = -\eta_{inv}(P_{dc} - B_t) + D, \quad (6)$$

where the value of self-produced PV energy is defined before the inverter. BESS discharge can be calculated using Equation (7):

$$G = \eta_{inv}(-B_t - P_{dc}) + D \quad (7)$$

### 2.2.2. Control of the Battery

When the BESS is used only to increase self-consumption of PV energy, controlling it is very simple. When surplus energy is available and the SOC is under the upper limit, the BESS is charging until either the SOC is at the maximum level or surplus energy is no longer available. It is better to discharge the BESS instantaneously so that the BESS can be ready to receive possible surplus energy in the future. Therefore, if the SOC is higher than the minimum limit and the demand of the customer is higher than PV production, the BESS discharges until either it is empty or PV production becomes higher than the demand.

### 2.3. Demand Response Operation

In this study, DR was implemented via a building's electric heating. The heat of electrical heaters can be stored in the mass of buildings and the air in rooms. Modern houses are better insulated, and they include heat storage, e.g., in concrete floors. If surplus PV production is available, the indoor temperature can be temporarily increased. Alternatively, if total consumption is required to be cut down, the indoor temperature can be temporarily decreased by interrupting the heating load. There are set values for the maximum changes in indoor temperature. Actual exact indoor temperatures cannot be known; therefore, they are modeled. Although this paper's focus is on electrical heating, the same method can be used when studying cooling systems or heating provided by heat pumps, but the efficiency of these other systems must be studied separately.

#### 2.3.1. Electrical Heating Systems and Theoretical Indoor Temperature

The load of electrical heaters depends on the outdoor temperature ( $T_{out}$ ), the value set for the indoor temperature ( $T_{set}$ ), and the stored thermal energy of the building. The building itself is similar to a form of energy storage, where the energy is stored as thermal energy. When  $T_{out}$  is lower than the indoor temperature ( $T_{in}$ ), the insulation of the building resists the self-discharge of the storage. Better insulation means lower self-discharge. The quality of insulation is represented by the total heat loss coefficient ( $c_f$ , W/K) of the building, which is the sum of the heat loss coefficients of different components of the building (roof, floor, etc.). The heat loss coefficient of the building's components can be calculated by multiplying the area ( $m^2$ ) of the components by the thermal transmittance (also known as U-value) of the material ( $W/m^2K$ ). The total heat loss coefficient of the building is defined by how much heating power is required to maintain a stable indoor temperature. A low heat loss coefficient is a valuable feature when pursuing low energy consumption. From the perspective of DR, a low heat loss coefficient means that the necessary flexibility must be obtained elsewhere because the ability to respond to demand is also low.

Buildings have a large mass that can store thermal energy. Heat can be stored in components such as concrete floors; however, all mass in insulations can store thermal energy. When the indoor temperature is constant, the energy stored in the mass does not change and it does not affect heating demand; however, when the indoor temperature changes, this stored energy strongly affects how fast heating demand changes. Every material has its own specific heat capacity ( $J/kg\cdot K$  or  $Wh/kg\cdot K$ ), and when we multiply it by the mass of the material, we obtain the heat capacity of the material. The sum of all heat capacities in a building is the total heat capacity ( $c_p$ , Wh/K) of the building. A large total heat capacity means that the indoor temperature changes gradually, e.g., after  $T_{set}$  changes or during heating power breaks, which are basic operations in DR. Total heat capacity is defined as the capacity to store thermal energy.

Changes in the theoretical indoor temperature can be calculated as follows using a building's total heat loss coefficient and total heat capacity [38]:

$$c_p \frac{dT_{in}}{dt} = E_h - c_f(T_{in} - T_{out}), \quad (8)$$

where  $E_h$  is heating power. This equation is derived from Newton's law of cooling. From Equation (8), we can solve the indoor temperature after the DR operation as

$$T_{in}(t) = T_{in}(t-1) + \frac{\Delta t}{C_p} [E_h(t-1) - c_f(T_{in}(t-1) - T_{out}(t-1))]. \quad (9)$$

Equation (9) can be used when modeling indoor temperature in scenarios in which heating power changes. Additionally, Equation (8) can be used when solving total heat capacity ( $c_p$ ) and the total heat loss coefficient ( $c_f$ ). When we have data regarding customer consumption and outdoor temperature, we can calculate  $c_f$  when we assume that indoor temperature is constant. Heating temperature ( $T_h$ ) is calculated using  $T_h = T_{in} - T_{out}$

–  $T_{self}$ , where  $T_{self}$  is the endogenous temperature from inside the building. It is typical that  $T_{set} = T_{in} = 21$  °C, but the building is required to be heated only when  $T_{out} < 16$  °C, which can be observed when comparing outdoor temperatures and heating demands. This difference results from small heat sources in the building. All electric devices incur heat losses when used, and people inside the building produce heat.  $c_f$  is defined using the measurement points  $E_h$  and  $T_h$ , where  $T_h > 0$ .  $c_f$  can be solved using the average value of heating power, which is divided by the heating temperature ( $c_f = \Sigma(E_h/T_h)/N$ ), where  $N$  is the number of measurement points. When we do not have exact measurements for heating power ( $E_h$ ), we use measurements of customers' total electricity consumption, though consumption which is in addition to that incurred from heating demand must be considered.

The other coefficient,  $c_p$ , can be solved similarly to  $c_f$ , but the difference is that now the change in temperature and heating power is studied over time. In DR operations, it is important to know how fast the indoor temperature changes when we modify heating power. Total heat capacity defines how fast this change is. If we do not have measurements for changes in indoor temperature, we can obtain total heat capacity when we know when and by how much the outdoor temperature changes. The same is applicable for changes in  $T_h$  if the changing component is  $T_{in}$  or  $T_{out}$ .  $c_p$  can be solved using the equation  $c_p = \Sigma(\Delta E_h/\Delta T_h)/N$ . The change in temperature and heating power can be increasing or decreasing. For the calculation, we selected hours when  $\Delta T_h > 0.5$  °C. Hours where the change was very small were ignored because this causes more errors than the amount of extra value gained for approximations. Other consumption causes random errors, but the error is minimal when using average values obtained with a high  $N$  value. Another reason is that the hysteresis curve for a thermostat, which controls the electric heaters, suffers from a higher amount of error with low temperature changes.

### 2.3.2. Simulation Model for Demand Response in a Heating System

In a DR operation, the indoor temperature is under control. In the simulations, the  $T_{set}$  of the building was 21 °C, and the approximation for  $T_{self}$  was 5 °C. This was an approximation based on consumption data, in which we noticed that heating demand frequently started to increase when the outdoor temperature decreased to under 16 °C. Additionally, we observed that average daily temperature ( $T_{Dave}$ ) affects heating demand. Even cold nights did not affect heating demand if  $T_{Dave}$  was over approximately 10 °C. In the simulations, heating began when  $T_{Dave}$  decreased below the building's daily average temperature limit for heating ( $T_{Dself}$ ). This  $T_{Dself}$  value varied significantly between customers; thus, it was calculated separately for every customer. The value of  $T_{Dself}$  can be determined by adjusting the value such that the amount of decreasing surplus energy is approximately the same as that in increasing self-consumption. With the wrong value, the simulation model does not work, and the simulated heating demand does not follow actual consumption data.

Stored heat is used and thus promptly restores the indoor temperature to the set value for two reasons. First, the system is again ready to receive surplus energy, and second, a higher indoor temperature causes slightly higher heat losses. In simulations, when a customer had a heating demand that was higher than the amount of PV production, the indoor temperature was promptly returned to the set value. Naturally, the total demand must not decrease below zero; therefore, heating demand can only decrease the amount of total load. In some cases, it will require several hours to reach the set value for indoor temperature after the DR operation.

The simulation model calculated the building's  $T_{in}$  every hour based on Equation (9) and coefficients  $c_p$  and  $c_f$ . The indoor temperature is assumed to be constant when either DR operations are not used or the outdoor temperature does not increase significantly. In summer, the outdoor temperature can become high even for long periods, which increases the indoor temperature. This is problematic for DR operations when they are used for storing surplus energy. High solar power production and high outdoor temperatures are

timed similarly, and there is naturally no heating demand where the surplus energy can be stored. When outdoor temperature increases to such a high value that  $T_h$  is negative, the indoor temperature increases based on Equation (9), and it can increase to very high values in simulations. In practice, customers may have cooling systems that decrease indoor temperatures and thus use some of the surplus energy in the process. These considerations are not involved in DR simulations because this demand can already be observed from the load profile and using the surplus energy to heat the building at the same time it is being cooled by the cooling system is pointless. Thus, the indoor temperature during the hot season demonstrates the building's potential to store heat more than it does the actual indoor temperature that customers can experience. Without the cooling system, the simulated indoor temperature corresponds to the actual indoor temperature, and when it is high, there is the potential to increase PV self-consumption with a cooling system.

#### *2.4. Combination of Demand Response and Battery Energy Storage Systems*

In simulations, DR operation and a BESS can be combined. These systems compete for the same surplus PV energy; therefore, it is assumed that these decrease each other's benefits. The combination is performed in two ways. First, DR is the primary operation, and if surplus energy remains, the BESS functions as a secondary operation. The other version is the opposite, where the BESS is the primary operation and DR is the secondary operation. In combined control simulations, the secondary operation does not affect the primary operation.

#### *2.5. Calculations with the Simulation Model*

The simulation model was formed by using MATLAB<sup>®</sup> code. Simulations utilized real hourly consumption data from customers and simulated new consumption profiles with the used components. The simulation period was an entire year. For the DR model, the total heat loss coefficient and total heat capacity were calculated separately for each customer. These coefficients were utilized in DR simulations where new customer consumption profiles were simulated with limited indoor temperature changes by using Equation (9). In BESS simulations, the new customer consumption profile was simulated by utilizing SOC changes in the BESS via Equation (3). Modeled PV production in simulations was calculated in hourly resolution from the results of Equation (1). The simulation model consists of many components which are modeled by using several references. Used methodologies are verified in the references. The code used for the simulator was carefully checked and tested before simulations.

### **3. Initial Data and Heating Coefficients**

#### *3.1. Electricity Consumption Data*

The study group consisted of 1525 customers in Finland. Customers were selected from a larger group (8078 customers) of one distribution system operator (DSO)'s customer base who had temperature-dependent loads, which means that they used electric heating systems. Temperature dependency is an important component that ensures these customers are suitable for studies involving the simulation of DR operation with electric heating. K-means clustering was used to select customers for this study group [39].

Consumption data were measured using the DSO's smart meters, and the same data were used when invoicing customer consumption. The data were measured in 2015, and consumption was metered hourly. We obtained 8760 data points from every customer, which were values for energy consumption per hour (kWh). Measurement accuracy was 0.01 kWh. The customers were located in rural areas or small towns in inner Finland. To protect the privacy of customers, the data are not being made public.

Additionally, data from one Finnish electrical heated detached house includes measurements for model validation that were made in 2022. Hourly measurements from the DSO's smart meters were used. For validation, indoor temperature was measured for a short time period.



### 3.2. Weather Data

Openly available data from the Finnish Meteorological Institute (FMI) were used for outdoor temperature data [40]. Temperature measurements were obtained for the area where the study group customers resided. Measurement accuracy was 0.1 °C. When the temperature is not measured immediately around the building, this causes an error in the results as there could be differences in temperature between locations even when they are very near to others. Nevertheless, the very accurate measurements of the FMI provided useful information about the temperature in the studied area.

### 3.3. Total Heat Loss Coefficient

Coefficients (total heat loss coefficient and total heat capacity) were defined separately for every customer. Figure 1 shows energy consumption per heating temperature throughout a year for one random customer. We can observe that the value was within a very narrow range in the heating season. There was no heating demand in the summer; therefore, the value decreased to zero. In spring and autumn, when the heating temperature was low, the range was higher because the weight of other consumptions increased. Consumption other than heating and daily changes in the load profile explain variations in the heating season. Consumption other than heating led to systematically higher total heat loss coefficient values. In Figure 1, the green line indicates the average value of the entire year, and the red line indicates the average of the heating season. The average value of the entire year was used in simulations because it better represents a base level of heating consumption. The load profiles of customers included all forms of consumption; therefore, other demands can be considered in addition to basic heating load, and from the perspective of this study, they are positive errors. For example, the total heat loss coefficient of 0.1 kW/K means that a 10 °C heating temperature causes an approximately 1 kW heating demand on average.

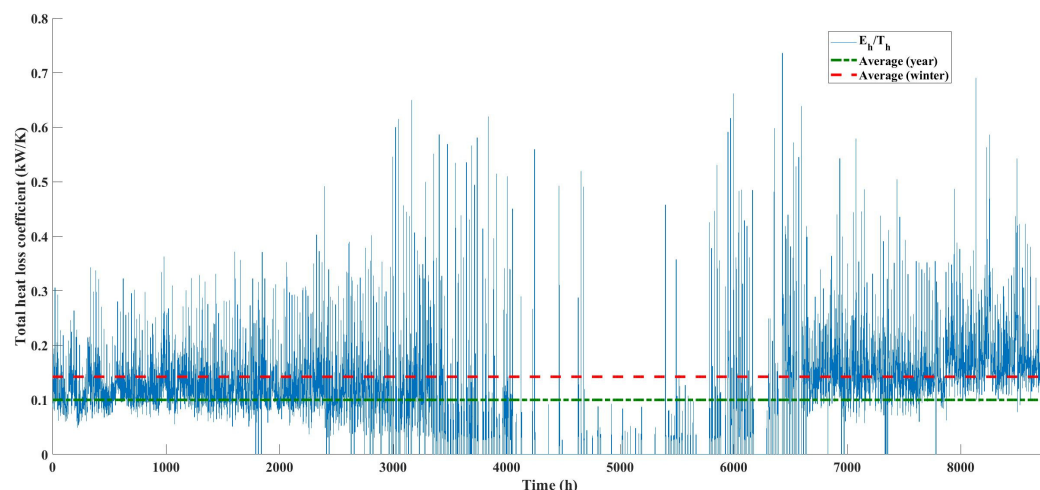


**Figure 1.** Total heat loss coefficient of a random customer. Heating time (winter) is outside of the June–August period (hours 3624–5808).

Figure 2 shows the calculated total heat loss coefficients for all customers. A few customers had a total heat loss coefficient that was very high or very low, but the value was approximately 0.1 kW/K for most customers. The average value of the total heat loss coefficient was 0.0937 kW/K for the entire group. Frequently, the heat loss of a building is calculated separately for each component. The size and materials of a building affect total heat loss. A very high total heat loss coefficient can be the result of a very large building or poor insulation. Some households in the study group could have had large sheds with poor insulation that were heated electrically. A very low total heat loss coefficient can mean that a building is very small with very good insulation and can also be the result of some buildings having their basic heating implemented in a manner that does not rely

on electrical heating (though they may have some extra electrical heating). Extremes are rare and approximately 91.5% of customers' total heat loss coefficients were in the range of 0.03–0.16 kW/K.

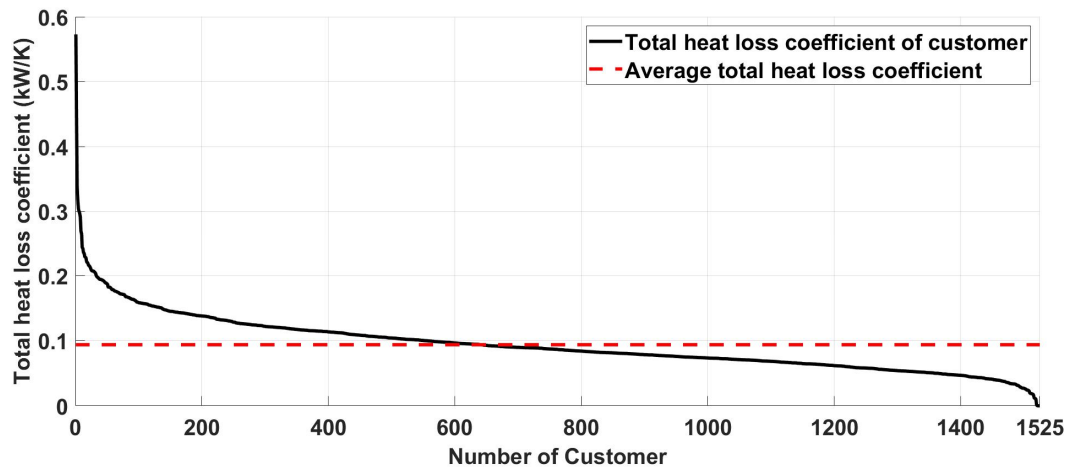


Figure 2. Total heat loss coefficients of customers in the study group.

### 3.4. Total Heat Capacity

Figure 3 shows the distribution of total heat capacity for a random customer. Every data point represents the change in consumption divided by the change in temperature over the same hour. Blue marks indicate a negative change, when consumption increased owing to decreasing outdoor temperature, and red marks indicate a positive change when consumption decreased due to increased outdoor temperature. Additionally, Figure 3 shows the average values of negative and positive changes and the average value of all changes, which were used as the total heat capacity of a customer in simulations. The variation was observed to be high. In summer, many low values caused high temperature changes with low heating demand. High values for the entire year were the result of changes in other forms of consumption with low outdoor temperature changes. The average value of the positive changes was slightly higher than the average value of negative changes because the increasing heating load caused higher heat loss. The average value of both changes provided a good estimate of the customer's total heat capacity. A total heat capacity of 1 kWh/K meant that the building could store as much heat as approximately 4800 kg of concrete.

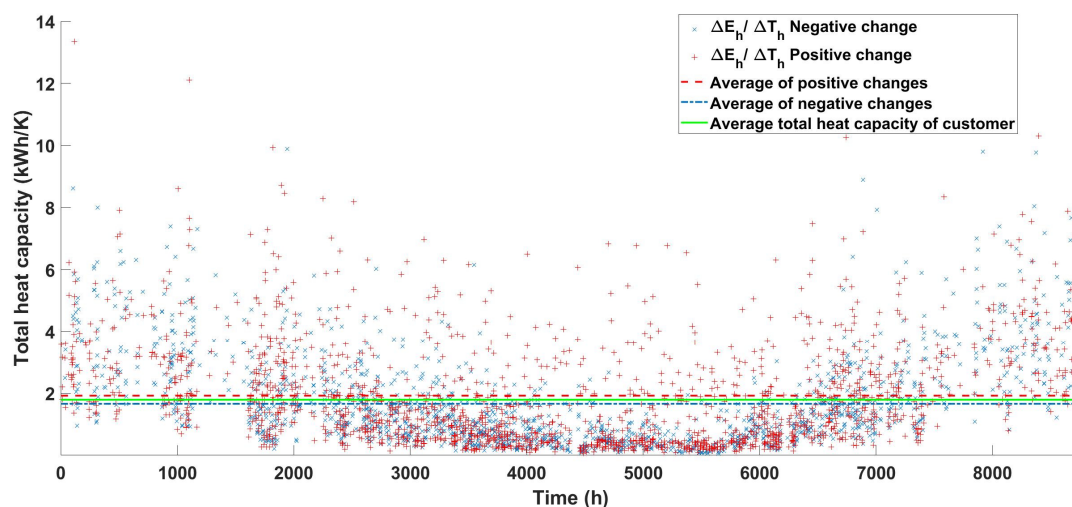


Figure 3. Distribution of total heat capacity for a random customer.

The total heat capacities of all customers in the study group are shown in Figure 4. The average total heat capacity of all customers was 1.7184 kWh/K. A few customers had very high total heat capacity and a few customers had very low total heat capacity. The majority, approximately 91.5% of customers, had a total heat capacity between 0.6 and 3.0 kWh/K. Total heat capacity values primarily depended on the size of the building and the construction materials used.

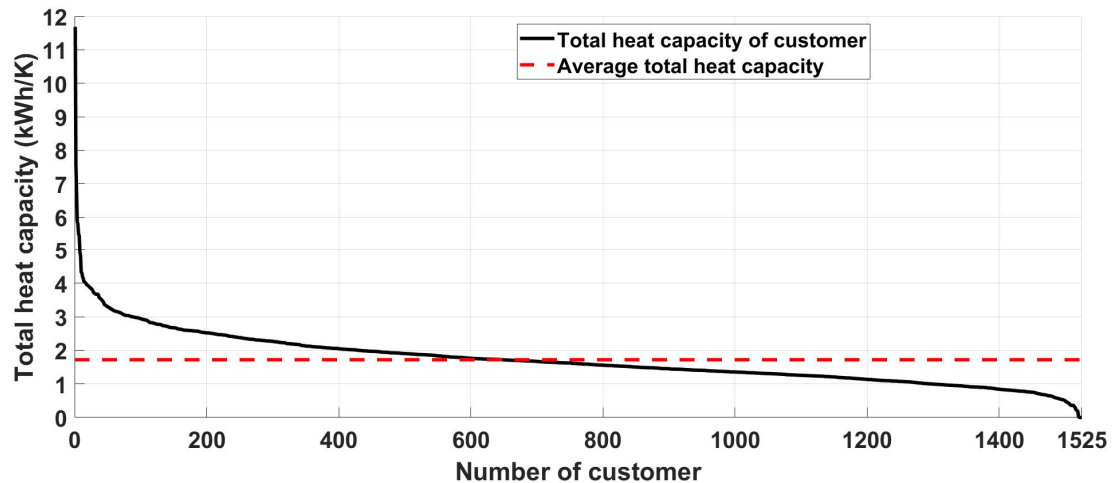


Figure 4. Total heat capacity for customers in the study group.

A building's total heat capacity depends strongly on its total heat loss coefficient, as shown in Figure 5. In most cases, both coefficients changed by the same proportion. In Figure 5, the linear regression line is indicated, which intersects the average total heat capacity line and average total heat loss coefficient line at the same point. Customers whose points are above the regression line had higher heat capacity in proportion to heat loss than average, e.g., modern well-insulated buildings have very low heat losses as they have a large mass that can store heat. A couple of surprising observations were that the calculated points were near the linear regression line and variation was very low, although the study group included buildings of different ages. The calculations indicate that all buildings with electrical heating have DR potential despite age or building type.

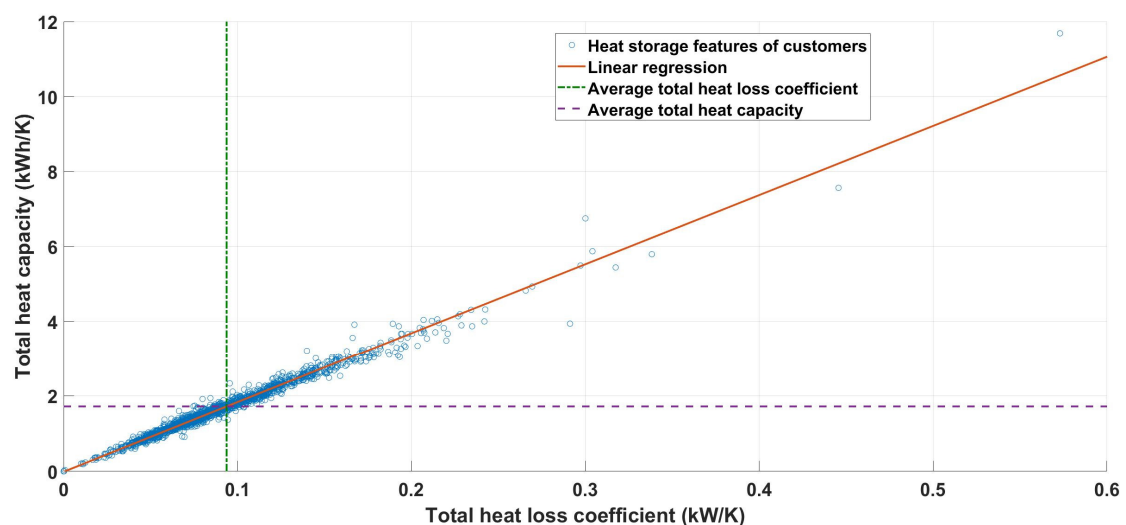
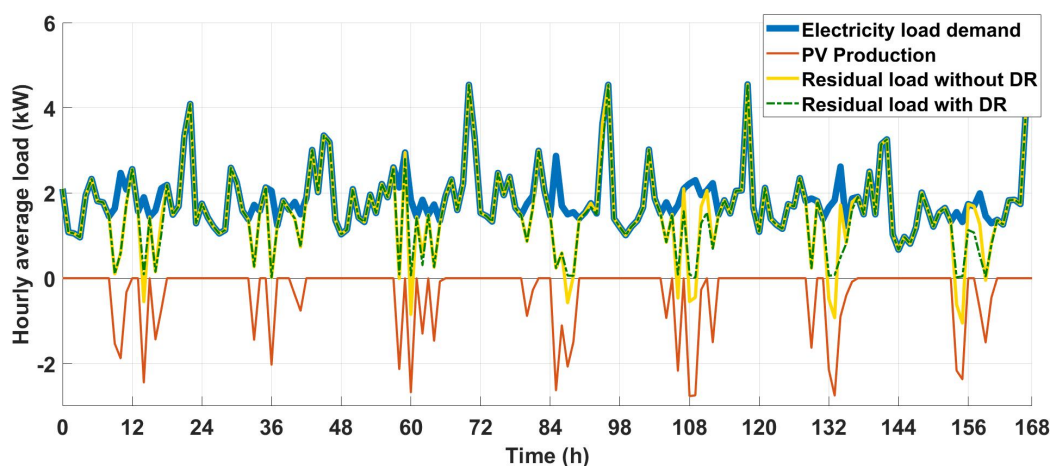


Figure 5. Customer heat storage features for demand response operations.

### 3.5. Example Case for Storing Surplus Energy in a Building

To demonstrate DR operation, we simulated a week's data (2–8 March) for a random customer with a 3 kWp PV system, and the results are shown in Figure 6. The blue line shows the customer's electricity consumption, and the red line shows PV production, which was negative because it has a decreasing effect in terms of total load from the grid's perspective. The yellow line is the total load, taken from the sum of consumption and production. We observed that the grid was fed for six days of the week, and this should be avoided for economic reasons. The outdoor temperature varied between  $-1.2$  and  $6$  °C during the week. The random customer's total heat loss coefficient was  $0.1$  kW/K and total heat capacity was  $1.7859$  kWh/K, i.e., very close to average values. The green line shows total load after the DR operation when all surplus energy was stored in the building's indoor heat. During this period, the indoor temperature varied between  $21.00$  and  $21.76$  °C, i.e., all surplus energy could be stored with a maximum increase in indoor temperature of only  $0.76$  °C. During this week,  $6.59$  kWh of surplus energy moved from grid feeding to self-consumption.



**Figure 6.** Storage of a random customer's surplus energy within the building over the course of a week.

### 3.6. Validation of the DR Model

Indoor temperature changes in DR operations were calculated as presented above. For validation, the changes in indoor temperature were measured in one typical electrically heated detached house in Finland. From the electricity consumption of this customer, the total heat loss coefficient was defined as  $0.1273$  kW/K and total heat capacity was defined as  $2.4559$  kWh/K. These values are slightly higher than in average buildings but are still close to the values of the main group of customers, as seen in Figure 5. The validation test was performed two times. In day 1, the test was timed so that electric heating was interrupted between 18:00 and 19:00, and in day 2 the period was 14:00–15:00. Indoor temperature was measured an hour before the interruption and two hours afterwards in 10 min intervals. Figure 7 presents the modeled and measured indoor and outdoor temperatures during the test period, so the interruption is timed between 1:00 and 2:00. In day 1, the outdoor temperature was about  $-6$  °C, and in day 2 it was around  $0.5$  °C. During these periods, there was a lot of other electric consumption that may have led to errors in modeling, and there were also other possible error sources such as outdoor openings which could thus affect indoor temperatures. Considering these error sources, the measured indoor temperatures follow the modeled indoor temperatures very well. This validation proves that the introduced simulation model also works in practice.

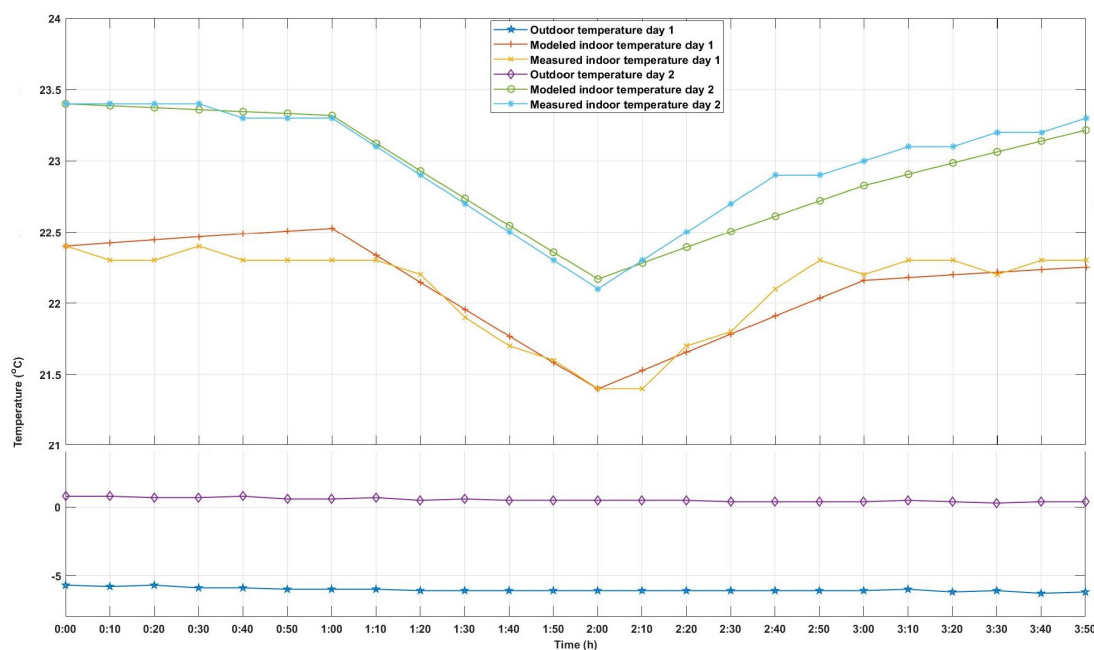


**Figure 7.** Validation of the DR model with temperature measurements. Scaling of the y-axis is divided in two different areas to show changes in values.

## 4. Simulations of Increasing PV Self-Consumption

### 4.1. Variable: Increase in Self-Consumption

With simulations, we studied the benefits that could be obtained with DR operations and the size of the BESS required for the same level of benefits. Additionally, we studied the possibility of using DR and a BESS together in the same building. The important question is whether the two technologies are competing against each other. To compare these technologies and their benefits, the increase in self-consumption (kWh) per year was a key variable. This was calculated as the average value of the decreased energy sold to the markets and the decreased energy purchased from the markets. Not all decreased energy sold to markets decreases the energy purchased from markets, as some of the energy is lost in heat losses in the DR operation. Therefore, the average value was the studied variable.

The increase in self-production is also a useful variable for studying BESS operations. The use of a BESS results in losses; therefore, the average value must be used, similar to DR. Because this variable is similar for both technologies, it can be used for comparison. We can first calculate the increase in self-consumption for DR operation and then determine the size of the BESS when the increase in self-consumption is similar.

### 4.2. Demand Response for Increasing Solar Power Self-Consumption

DR operations were studied with two different sizes of PV systems, which were 3 and 6 kWp. These sizes correspond to the typical sizes of PV systems in detached houses [4]. The smaller 3 kWp system is a traditional size in which grid feeding is avoided, and the larger 6 kWp system is an economically optimal size for PV systems. The exact optimal size must be determined separately for every customer using an electricity pricing model, but a constant size was used to make the results comparable. Two different levels of DR operations were studied: the indoor temperature could increase by a maximum of either 1 or 2 °C from a basic level of 21 °C. The results are presented in Figure 8, where customers are arranged in order of size according to the increase in the self-consumption. A few customers had a much higher increase in self-consumption than others, but the majority of the study group had very similar results.



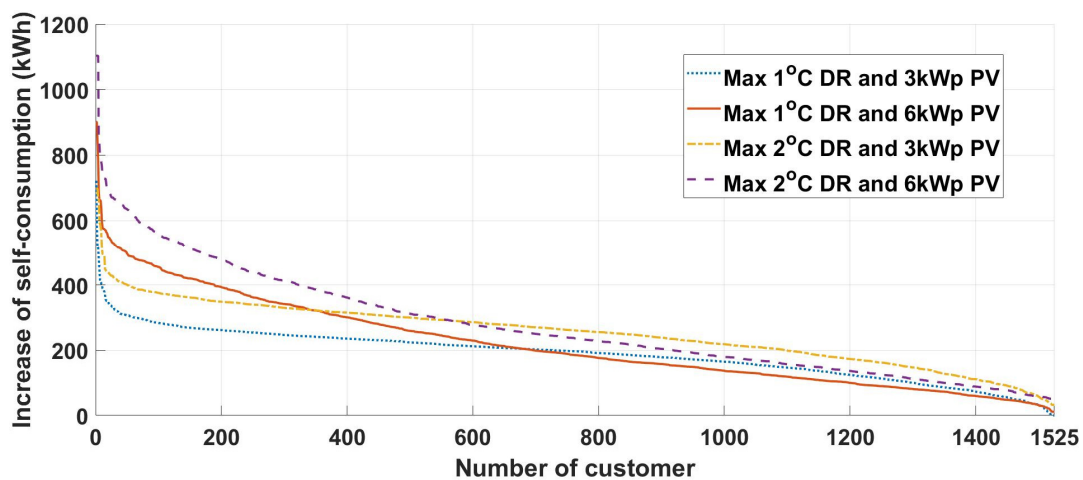


**Figure 8.** Effect of total heat capacity on customers' increased self-consumption at two different levels of DR operation and with two different PV panel sizes.

The average yearly increase in self-consumption with 3 kWp PV panels was 187.5 kWh with a maximum DR of 1 °C and 252.5 kWh with a maximum DR of 2 °C. When a 6 kWp PV system was used, the average values were 217.6 kWh with a maximum DR of 1 °C and 273.4 kWh with a maximum DR of 2 °C. The shapes of the curves in Figure 8 show that a group of customers (approximately 600 customers) received higher benefits from the DR operation with the 6 kWp PV system than with the 3 kWp PV system. These customers' load profiles facilitated the storage of surplus energy from the larger PV system as heat in the building. Other customers could not receive higher benefits from DR with a larger PV system. The increase in self-consumption for these customers was lower with the 6 kWp PV system than with the 3 kWp PV system because the larger PV system resulted in lower consumption in the load profile, which could thus be fulfilled from the stored heat. For clarification, Figure 9 shows annual PV production with 3 kWp and 6 kWp systems and customers' total consumption when they are ordered similarly to how they are in Figure 8. Total consumption affects the increase in self-consumption, but there is also a lot of variation because the customers' thermal coefficients and load profile affect the results.

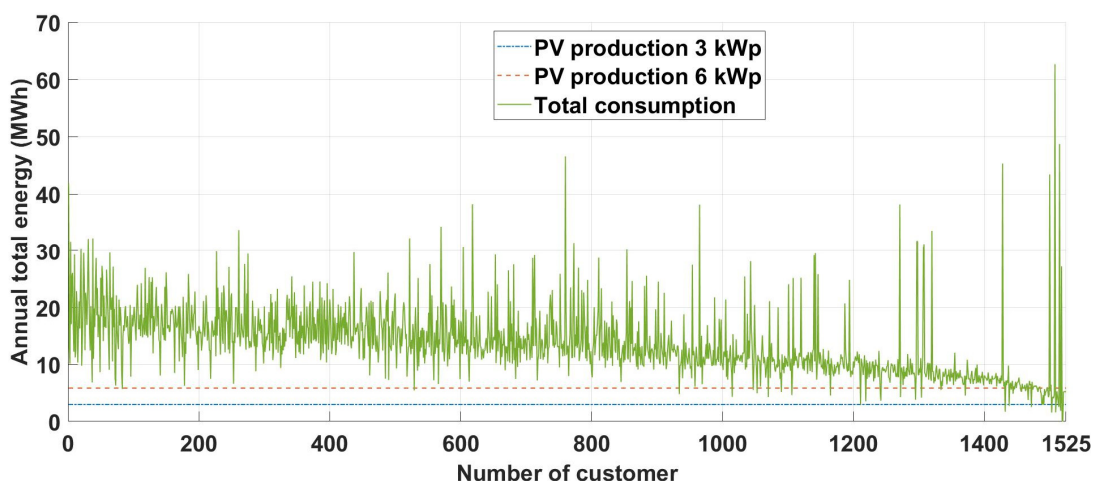


**Figure 9.** Annual PV production with 3 kWp and 6 kWp systems and the total consumption of customers. Customers are in the same order as they are in Figure 8.

When the DR limit increased from 1 to 2 °C, all customers gained more benefits with both PV sizes, but the increase due to a 2 °C increase was much lower than that of a 1 °C increase. The increase in self-consumption from the 2 °C increase was only 0.35% with the

3 kWp PV system and 0.26% with the 6 kWp PV system when compared to the increase in self-consumption that resulted from a 1 °C increase. When indoor temperature variation increased, it caused more discomfort for customers and the increase in benefits decreased; therefore, the limits for indoor temperature variation must be selected wisely.

We studied the effects of the features of customers' buildings on the increase in self-consumption. Figures 10 and 11 show the same results, but the x-axis shows the customer's total heat loss coefficient in Figure 10 and the customer's total heat capacity in Figure 11. Both features affected increases in self-consumption in a similar manner. An approximately 0.1 kW/K total heat loss coefficient and 2 kWh/K total heat capacity were the limit values that divided customers into those who received higher benefits from DR operation with the larger PV system and those who did not. The results indicated that the higher total heat loss coefficient and higher total heat capacity provided customers with higher benefits from the DR operation, though limits existed at which benefits no longer increased. A small group of customers obtained clearly higher benefits from the DR operation with a low total heat loss coefficient and low total heat capacity. These customers had low base consumption but repeated high load peaks, which caused systematic errors in the simulation results.

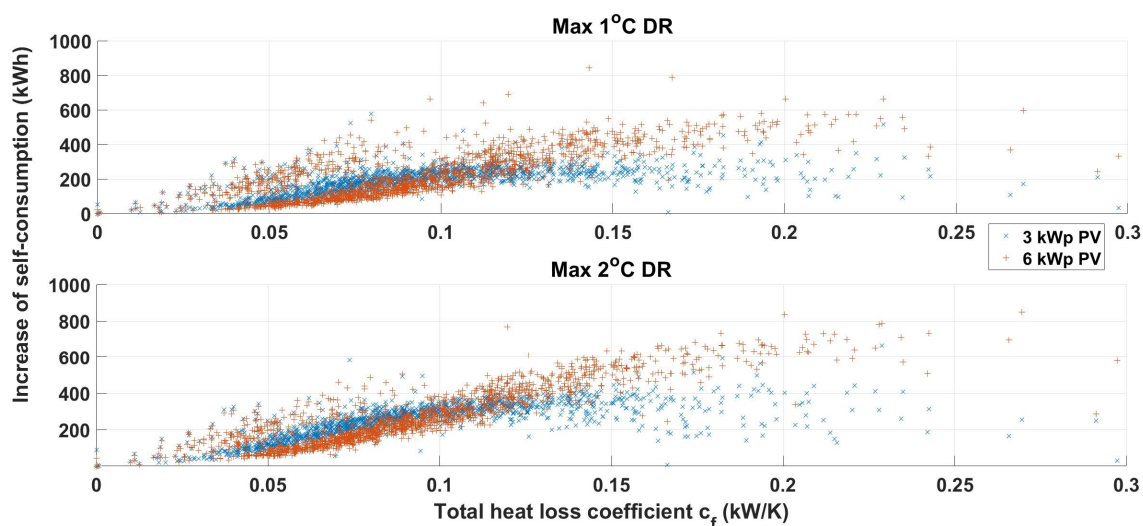


**Figure 10.** Effect of total heat loss coefficient on customers' increase in self-consumption at two different DR operation levels and with two different sizes of PV panels.

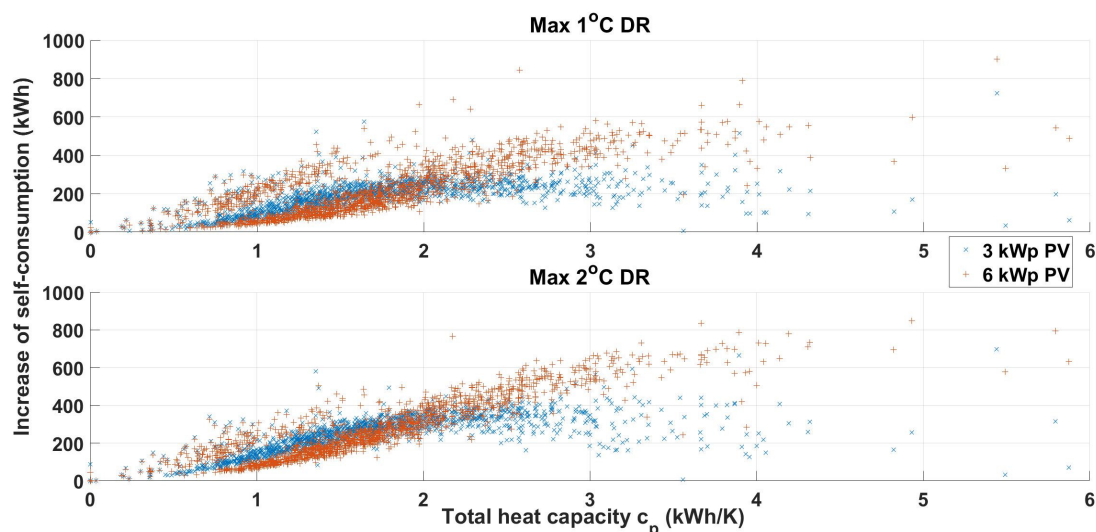


**Figure 11.** Effect of total heat capacity on customers' increase in self-consumption at two different DR operation levels and with two different sizes of PV panels.

#### 4.3. Comparison of Demand Response and Battery Energy Storage

The results of the DR operations indicated the value of the increase in self-consumption, and the aim of the BESS simulations was to determine the size of the battery when the increase in self-consumption was similar to that of the DR operation. The initial battery size was set to 100 Wh and if the increase in self-consumption was lower than that of the DR operation, the size of the battery was increased in 10 Wh increments until the increase in self-consumption was a maximum distance of 5 kWh away from the value of the DR operation. The results for all four cases are shown in Figure 12. A few customers required a higher storage capacity to reach a similar increase in self-consumption to that of the DR operation, but the main research group required only a very small storage capacity in this regard. The average values for battery sizes corresponding to DR operations were a maximum of 1 °C DR and 0.83 kWh when the PV system size was 3 kWp and 0.65 kWh when the PV system size was 6 kWp. Under DR operations, the indoor temperature could increase by a maximum of 2 °C, and the average values were 1.67 kWh with the 3 kWp PV system and 0.91 kWh with the 6 kWp PV system. The smaller PV system required a higher BESS capacity on average to reach a similar increase in self-consumption to that achieved with DR. The reason for this is that the BESS must use a large amount of energy with the 3 kWp PV system to reach the set increase in self-consumption because the amount of surplus energy is low. With the 6 kWp PV system, the amount of surplus energy is large, and the BESS could thus be used efficiently.

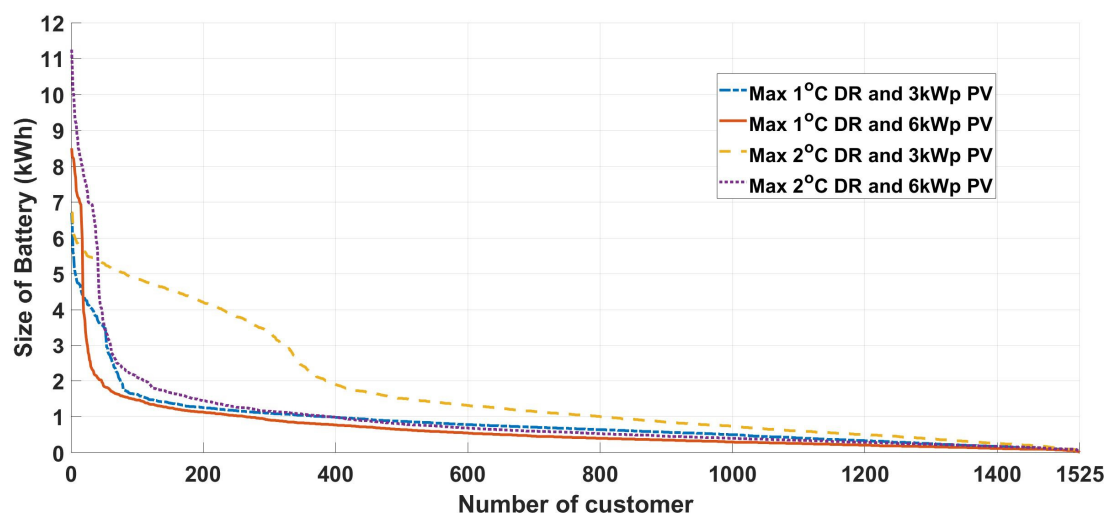


**Figure 12.** Battery sizes required to provide the same increase in self-consumption to that of DR operations at two different DR levels and with two different PV panel sizes.

The curves of these cases appear to be very similar, except in the case of a maximum of 2 °C DR with the 3 kWp PV system, which is quite different to the others. This inconsistency required further close study. Therefore, Figure 13 shows the results for battery size (x-axis) and increases in self-consumption (y-axis), which was used to define the battery size. We can observe that with a maximum of 2 °C DR and a 3 kWp PV system, a large group of customers required high battery capacity (3–6 kWh) to reach an approximately 300–400 kWh increase in self-consumption. These values representing increases in self-consumption were the maximum values for these customers that could be reached with the BESS or DR, and this value was more difficult to attain with BESSs because BESSs cause more losses than DR. In simulations, DR caused only negligible losses with a maximum 1 °C and maximum 2 °C indoor temperature change, while BESSs caused significant losses. These customers were not valid for the comparison study between DR and BESSs with the 3 kWp PV system, but this result indicated the importance of sizing the PV system and the BESS correctly for the load profiles of customers. Additionally, Figure 13 shows that the increase in self-consumption increased rapidly when the size of the battery increased, but

there was a clear limit at which the increase stopped. With the 3 kWp PV system, this limit was approximately 200–400 kWh, and with the 6 kWp PV system, it was approximately 500–700 kWh. Most customers could reach this limit with a very small BESS size. With the 3 and 6 kWp PV systems, the BESS size was approximately 1 and 2 kWh, respectively. These results show that, for sizing the BESS, the 2 kWh capacity is suitable in most cases.

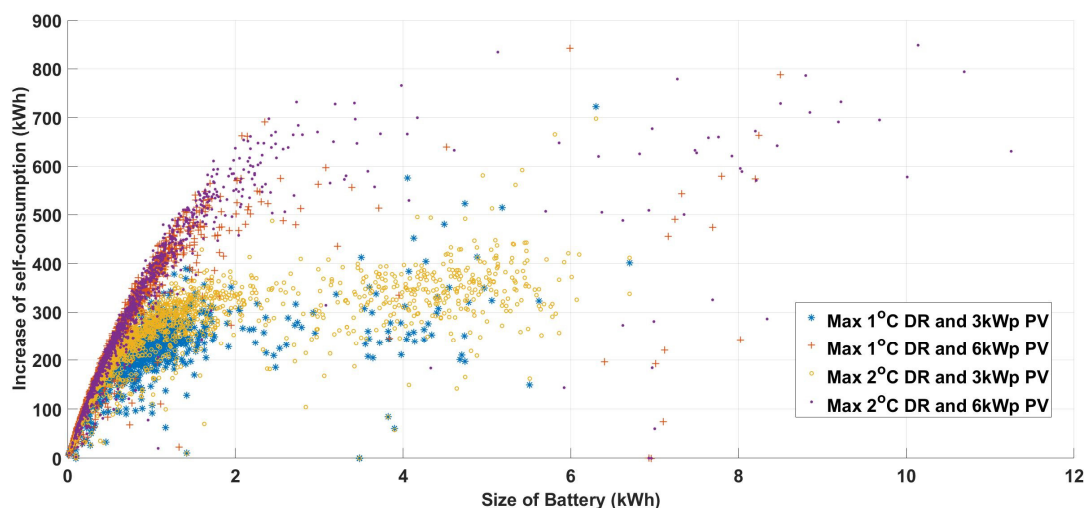


**Figure 13.** Battery sizes which provide the same increase in self-consumption as DR operations at two different DR levels and with two different PV panel sizes.

#### 4.4. Using Demand Response and Battery Energy Storage Together

One of the main research questions in this study was whether the DR and BESS operations compete against each other. Is it possible to use both controls simultaneously such that one does not impair the other's potential? The use of DR and BESS together was studied with a 2 kWh BESS and a DR operation in which the indoor temperature could change by a maximum of 1 or 2 °C. This combination can be implemented by using the DR operation as the primary control and then using the BESS under surplus energy as the secondary control, or vice versa. The potential of DR depends on the demand for heating power; therefore, the DR is only rarely available. If the BESS is the primary control, the amount of time slots where DR can be used can decrease, and if the DR operation is primary, the possibilities for using the BESS can decrease. It is very interesting to compare which primary control is more disadvantageous than the other. The results of these combination simulations can be compared to the sum of results from separate simulations of DR and BESS operations.

The results of the comparison are presented in Figures 14 and 15, which show the results for a maximum 1 and 2 °C DR, respectively. Two different PV system sizes (3 and 6 kWp) were used; therefore, the initial settings formed four different variations (two DR levels and two PV sizes). With every variation in settings, we simulated four different cases: primary controls with DR and a BESS and the secondary controls of both. The secondary controls were simulated using the results of primary controls as the initial load profile. Thus, in the results, the combination controls were the sums of the results from the primary and secondary controls. The case in which DR was primary and the BESS secondary is denoted as DR&BESS, and the case in which the BESS was primary and DR secondary is denoted as BESS&DR. For comparison, the sum of both primary controls DR+BESS, which represents the theoretical maximum, is also shown.

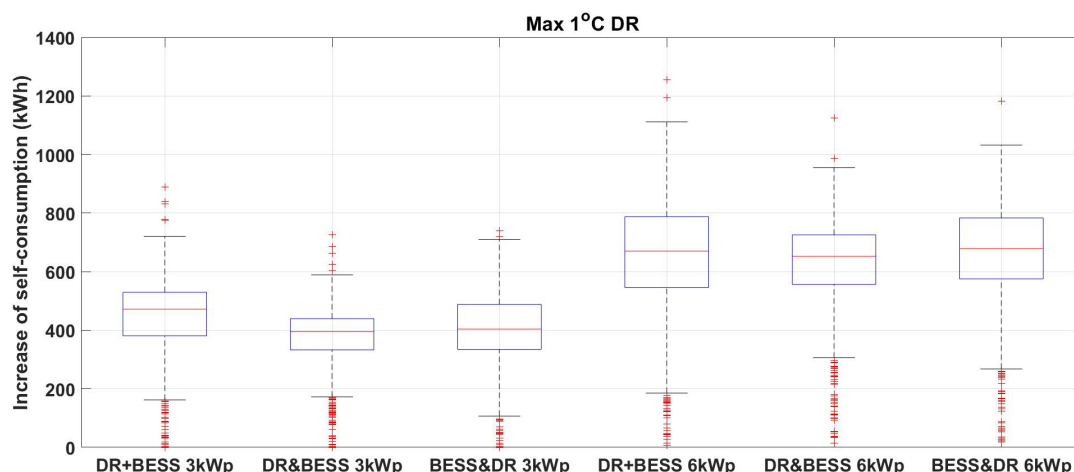


**Figure 14.** Comparison boxplot of customers' increase in self-consumption with a maximum 1 °C DR and a 3 or 6 kWp PV system. The results from both (BESS and DR) separate controls are summarized as DR+BESS, combined controls where the DR is the primary control and the BESS is the secondary control are summarized as DR&BESS, and combined controls where the BESS is the primary control and DR is the secondary control are summarized as BESS&DR. The boxplot shows the median, and the bottom and top edges of the box indicate the 25th and 75th percentiles, respectively.

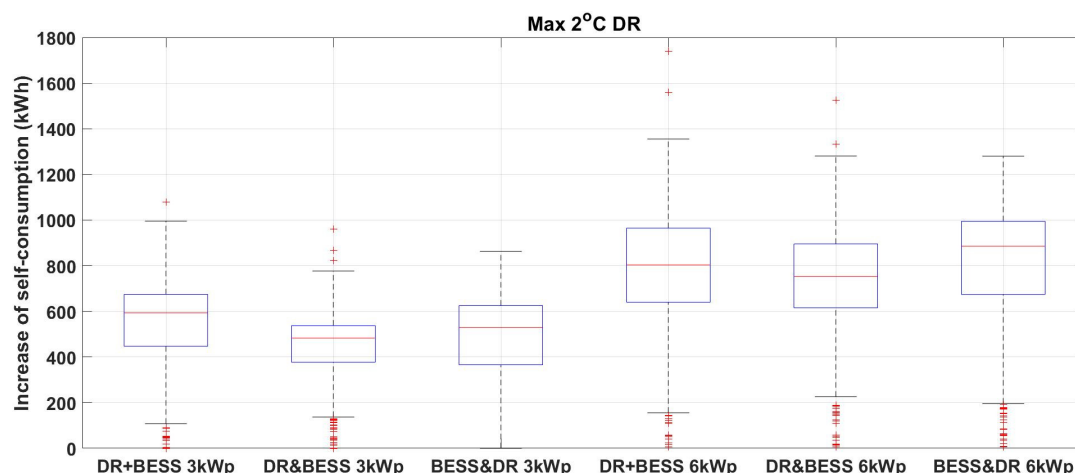


**Figure 15.** Comparison boxplot of customers' increase in self-consumption with a maximum 2 °C DR and a 3 kWp or 6 kWp PV system. The results from both (BESS and DR) separate controls are summarized as DR+BESS, combined controls where the DR is the primary control and the BESS is the secondary control are summarized as DR&BESS, and combined controls where the BESS is the primary control and the DR is the secondary control are summarized as BESS&DR. The boxplot shows the median, and the bottom and top edges of the box indicate the 25th and 75th percentiles, respectively.

The results from all cases and variations in settings clearly show that DR and BESS operations can be used together. When the PV system size was 3 kWp, the combination controls produced a lower increase in self-consumption than the sum of separate controls, but the difference was very low. When the size of the PV system doubled to 6 kWh, the differences were even lower because more surplus energy was then available. A surprising result was that with a maximum 2 °C DR level and 6 kWp PV system size, the combination BESS&DR had an even higher median value than the sum of separate controls. The reason for this was the limitations placed upon the DR operation. The capacity and requirement for DR operation was constantly changing when the outdoor temperature and PV production changed continually. The same fluctuation in indoor temperature resulted in different



increases in self-consumption when the BESS operation was performed first and a large amount of surplus energy remained, and the required DR operations may be more suitable from the perspective of increasing self-consumption than cases without the BESS. This enables some cases of the BESS&DR combination to produce a higher increase in self-consumption than the theoretical summation of both controls (DR+BESS). Even the exact increase in self-consumption depends on the load profile of the customer; these results show clearly that if DR and BESS operation are used simultaneously, it is better to use the BESS as the primary control and DR as the secondary control.

### 5. Analysis of Demand Response Potential in the Grid

In the simulations, we studied individual customers' potential to store surplus PV production through DR or BESS operations. Additionally, the presented method enables us to evaluate DR possibilities in large groups of customers. If customers' DR potential were centrally controlled, it could be utilized for everyone's benefit, e.g., a DSO could avoid high peaks or an energy retailer could shift load to cheaper hours. There are two main questions for the DR potential of the customer group. First, how much flexible power is available? Second, how long can the load flex? The heating power of flexible buildings depends on the outdoor temperature; thus, it varies significantly. Figure 16 shows the total hourly heating power of the entire 1525 customer group, which is the flexible power that can be cut in a centrally controlled DR operation if required. This depends on the outdoor temperature; therefore, the temperature limits are presented in Figure 16. In the geographical area where the studied customers lived in 2015, there were 1960 h where the outdoor temperature was below 0 °C, and the heating power of the study group was at least 2.3 MW. This is the power that can be cut by interrupting electric heating in these buildings. For the coldest hour of the year, heating power was 5.7 MW, which was the maximum DR capacity.

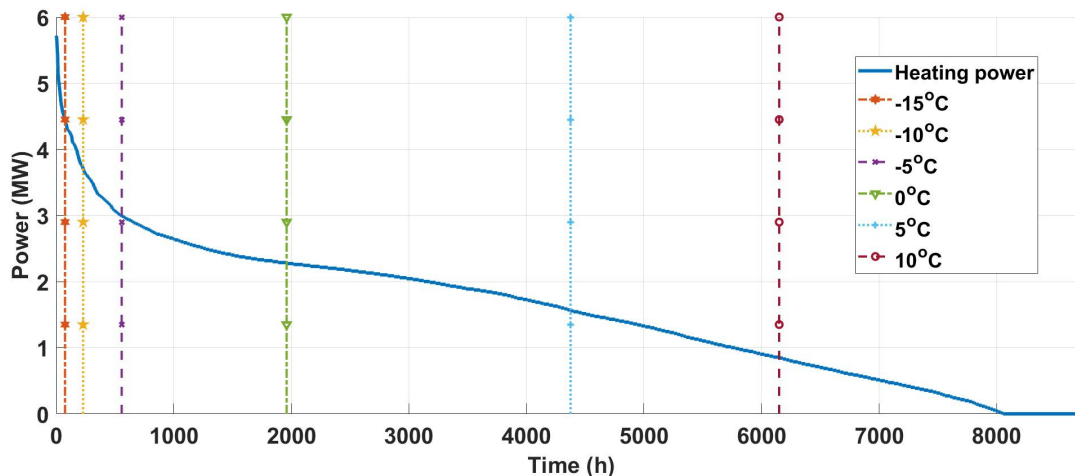


**Figure 16.** Total heating power of all 1525 customers in the study group for every hour of the year in descending order with six dashed lines corresponding to different outdoor temperatures.

The question of how long the heating load could be interrupted also needed to be answered. This question was answered by studying the decreasing indoor temperatures in the studied buildings. The initial temperature was set to 21 °C in all buildings, and the heating was then interrupted for an hour. Figure 17 shows the percentage of customers that could allow their heating power to be interrupted without the indoor temperature decreasing by more than the DR limit at any hour of the year. There were four DR limits, which were 2, 1.5, 1, and 0.5 °C. If indoor temperature decreased by a maximum of 2 °C, there were 8535 h of the year where 100% of customers could tolerate a maximum of an hour of heating power interruption. This also means that only 225 h in 2015 were very cold (under −15 °C), and that only some customers' indoor temperature decreased by more than

2 °C during the hour-long heating power interruption. If the DR limit is tighter, the amount of hours where all customers can tolerate heating power interruption is much lower.

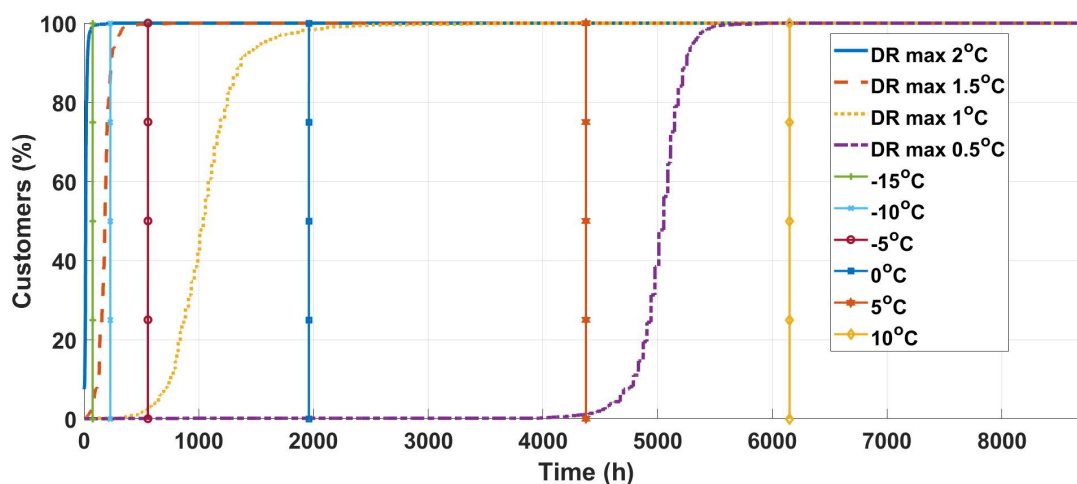


**Figure 17.** Percentage of customers whose indoor temperatures do not decrease by more than the DR limit (2, 1.5, 1, and 0.5 °C) during an hour-long heating power interruption. The hours of the year are sorted in ascending order by outdoor temperature and the six vertical lines correspond to different outdoor temperatures.

Figure 17 shows that when the outdoor temperature is very cold, a customer's indoor temperature can decrease rapidly. However, approximately 7% of customers were able to tolerate an hour-long heating power interruption (less than a 2 °C decrease in indoor temperature) during the coldest hour of the year. When the results in Figures 16 and 17 are examined together, we can observe when flexibility is available with different DR limits. If the DR limit is a maximum of 1 °C for an outdoor temperature of 0 °C, approximately 2.3 MW of flexibility is available; however, when the outdoor temperature decreases, the amount of flexibility decreases rapidly (even when heating load increases), as customers do not tolerate any more interruption to heating power.

## 6. Discussion

The motivation for this study was a comparison between DR operations and battery operations. The approach toward studying DR operations implies that studies with few modeled buildings are insufficient in terms of sample size. In battery operations, the load profile of the customer is strongly affected; therefore, variations in load profiles must be widened in research. This approach provides a novel method for studying the DR potential of a large study group. This method requires only weather and consumption data, which makes it very useful. Knowledge of customers' heating systems or building sizes or types is not required. Aggregators who offer DR operation services can approximate the DR potential of customers using this method. This method is also very useful for researchers because it facilitates many future studies, e.g., coefficients of customers' heating features could be used to form load forecasting models or approximations of the DR potential of all buildings in a studied area. Coefficients defined from historical data can be used for forecasting customers' heating load with forecasted temperatures.

In this study, the comparison of DR and battery operations focused only on increasing PV self-consumption, and only heating demand was used in the DR operation. These two selections were made for multiple reasons. Increasing PV consumption is the most used control target for batteries and is available to most customers, while also being more profitable in most cases [41]. Additionally, the combination of different control targets causes a loss of benefits due to inaccurate load forecasts. The use of different control targets is a topic that could be explored in future research.

DR operations have multiple load types that can be used. In many studies, domestic hot water boilers have been controlled by DR operations, e.g., in [17]. It is a natural target for DR operations because it includes thermal storage with a known capacity, and heating requirements can therefore be modeled. It is widely studied, and this possible DR capacity must be remembered when analyzing the results of this study. However, only the total consumption of customers is widely metered, and the load of a hot water boiler is one part of these measurements. These loads do not follow the outdoor temperature and depend on the customer's behavior, such as the use of other devices, washing machines, or electric saunas, which are also good objects for a DR operation. Therefore, the electric heating of a building is the only target for a DR operation that can be directly detected from total consumption measurements, which is achieved by comparing consumption and temperature measurements.

Only customers whose consumption followed the outdoor temperature were selected in the study group because these customers were known to use electric heaters. No exact knowledge was derived regarding customers' heating systems; therefore, this group could also include customers with electric heaters that are used as secondary heating systems, e.g., heated floors in wet rooms. This could result in a scenario where, if secondary heating is under DR operation, the primary heating system compensates for it. Additionally, customers with electric heaters as their primary system could have a secondary system, e.g., a fireplace. These can cause errors in results, but because the proposed method examines the load profile of an entire year, the effect of these errors is minimal. If a customer systematically uses another heating source when the outdoor temperature is very low, the method observes this, and the coefficient of heat loss decreases; thus, it is indicated in DR capacity approximations.

The indoor temperature of buildings is modeled and does not correspond exactly to the actual indoor temperature. Many behaviors by customers affect indoor temperatures (e.g., door openings), and not every customer sets their indoor temperature to 21 °C. Therefore, these factors cause errors in the results. In DR simulations, the changes in customers' heating loads are adjusted such that their measured load profile follows the changes in indoor and outdoor temperature. Hence, the modeled indoor temperature is only a variable in simulations, and it does not correspond exactly with the actual indoor temperature level. Only the changes in indoor temperature are relevant. When the number of measurement points is high (8760 per year) and errors occur in both directions, the errors can be minimized in the long term by using mean values.

The proposed method is based on direct electric heaters where heating load depends linearly on the outdoor temperature. Direct electric heaters are controlled by a thermostat. The hysteresis curve of thermostats causes lag for heaters reacting to changing temperature. This lag causes errors when defining the total heat capacity of a building because the response of electric heaters is slow. This error is minimized by using only hours where temperature change is high, because then the effect of lag is negligible with a simulation time step of one hour. If customers have heat pumps, dependency between outdoor temperature and heating load is no longer linear because of heat pumps' temperature-dependent efficiency. If this method is used with heat pump customers, the heating load indicates the direct thermal heat energy demand of the customer, and the efficiency of the heat pump must be considered as a correlation coefficient.

On a large scale, DR capacity is an interesting aspect when high flexibility is required, e.g., when large power plants rapidly disconnect from the power grid. The use of reserve power plants can be avoided if customers can be flexible in these scenarios and decrease their consumption. The present study demonstrates how long 1525 customers were able to be flexible in these scenarios and the degree of flexibility they had. These customers were grouped in an area containing a total of 8078 customers. This means that approximately 19% of the customers in this area were able to implement this flexibility. In the heating period, DR potential varies hourly from 15% to 30% of the total consumption of all customers (average of approximately 20%), i.e., the DR potential of electric heaters can rapidly cut

approximately 20% of the total consumption of all customers. The percentage varies hourly owing to changes in the outdoor temperature and total consumption. The statistics from 2020 show that Finland has 589,106 electrically heated buildings, which means approximately 38% of all buildings [42]. Therefore, small-scale customers can develop high DR potential in Finland.

Although this study was conducted with Finnish data, the results are applicable anywhere electric heaters are used to heat buildings. Additionally, the method for obtaining the heating coefficients of buildings can be used with cooling systems. If electricity load follows the outdoor temperature, this method can be used to approximate a building's capacity for storing energy in cold as well as hot conditions.

## 7. Conclusions

The DR features of electrical heating systems in small-scale residential buildings can be determined from electricity consumption data. The total heat loss coefficient and total heat capacity are the key coefficients when studying the effect of heating load DR on a building's indoor temperature. These coefficients can be estimated by comparing outdoor temperature and a building's consumption data. Without knowledge of a building's actual indoor temperature, the coefficients can be estimated by comparing changes in outdoor temperature and customers' load profiles. This novel method uses changes in loads and outdoor temperatures over time as they are the same for mathematical models of thermal features with changing variables for indoor or outdoor temperatures (the effective variable is the difference between them).

The presented novel method for evaluating the DR possibility of electric heating fulfils the outlined objectives. The advantages of the method are that it is simple and requires only minimal information. It is suitable for quickly evaluating the DR potential of large customer groups. Earlier methods need specific information about the thermal features of a building's materials, and these methods provide a rough estimate which should be verified afterwards. These methods are well suited to new buildings. The presented novel method is not suitable for new buildings because history consumption data are needed. This novel method is very effective with old buildings and makes it possible to evaluate the existing building stock.

The DR operation of an electrical heating load or a battery can be used to increase PV self-consumption. The capacity of a DR operation is quite low for individual small-scale customers, and its effectiveness corresponds to battery capacity. Most of the benefits can be obtained from the flexibility acquired with one degree temperature changes, and when the indoor temperature fluctuates by more than one degree, the benefits do not increase as rapidly as comfort is lost. Thus, for increasing PV self-consumption, it is effective to use low flexibility limits.

With an effectively sized DR operation and battery system, both can be used simultaneously without much of the benefit being lost. Both methods compete to utilize the same surplus PV energy; however, with an optimally sized PV system, surplus energy remains for both methods. When combining both methods, it is more profitable to use battery systems as the primary control and DR operation as a secondary control.

Customers' heating loads can be used in centrally controlled DR operations when it is possible to temporarily decrease the total consumption of customers by a significant amount. This type of operation can aid the power system in scenarios in which production rapidly decreases or high consumption peaks in the grid need to be avoided locally. The problem is that during very cold outdoor temperatures when consumption is typically highest, the indoor temperature of residences decreases rapidly during heating load interruptions, which limits the amount of time that customers can be flexible.

The results of this study will benefit many future studies. The method of defining the DR potential of small-scale customers can be used when studying the DR potential of larger areas involving higher numbers of customers. Future research should investigate different control targets for comparison to the proposed DR and battery system. Electricity market

price levels and variation have been increasing significantly since autumn 2021 because of difficulties in energy markets. There could therefore be significant potential in market price-based control, which should be researched more in future. Additionally, different loads as the target of DR operation will be the object of future research.

**Author Contributions:** Conceptualization, J.K.; methodology, J.K.; software, J.K.; validation, J.K.; formal analysis, J.K.; investigation, J.K.; resources, J.K. and P.J.; data curation, J.K.; writing—original draft preparation, J.K.; writing—review and editing, J.K. and P.J.; visualization, J.K.; supervision, P.J.; project administration, P.J.; funding acquisition, P.J. All authors have read and agreed to the published version of the manuscript.

**Funding:** This research was part of the Analytics project funded by the Academy of Finland and the PRELUDE project funded by the European Union’s Horizon 2020 research and innovation programme under Grant Agreement N° 958345.

**Data Availability Statement:** Original data are not available for the protection of electricity users’ privacy.

**Acknowledgments:** The authors wish to thank the funders, partners, and supporters for enabling the use of data that were necessary for this study.

**Conflicts of Interest:** The authors declare no conflict of interest.

## References

- Child, M.; Kemfert, C.; Bogdanov, D.; Breyer, C. Flexible electricity generation, grid exchange and storage for the transition to a 100% renewable energy system in Europe. *Renew. Energy* **2019**, *139*, 80–101. [\[CrossRef\]](#)
- Paterakis, N.; Erdinç, O.; Catalão, J.P.S. An overview of Demand Response: Key-elements and international experience. *Renew. Sustain. Energy Rev.* **2017**, *69*, 871–891. [\[CrossRef\]](#)
- Dietrich, A.; Weber, C. What drives profitability of grid-connected residential PV storage systems? A closer look with focus on Germany. *Energy Econ.* **2018**, *74*, 399–416. [\[CrossRef\]](#)
- Koskela, J.; Rautiainen, A.; Järventausta, P. Using electrical energy storage in residential buildings—Sizing of battery and photovoltaic panels based on electricity cost optimization. *Appl. Energy* **2019**, *239*, 1175–1189. [\[CrossRef\]](#)
- Andreolli, F.; D’alpaos, C.; Moretto, M. Valuing investments in domestic PV-Battery Systems under uncertainty. *Energy Econ.* **2022**, *106*, 105721. [\[CrossRef\]](#)
- Merei, G.; Moshövel, J.; Magnor, D.; Sauer, D.U. Optimization of self-consumption and techno-economic analysis of PV-battery systems in commercial applications. *Appl. Energy* **2016**, *168*, 171–178. [\[CrossRef\]](#)
- Aniello, G.; Shamon, H.; Kuckshinrichs, W. Micro-economic assessment of residential PV and battery systems: The underrated role of financial and fiscal aspects. *Appl. Energy* **2021**, *281*, 115667. [\[CrossRef\]](#)
- Angenendt, G.; Zurmühlen, S.; Axelsen, H.; Uwe Sauer, D. Comparison of different operation strategies for PV battery home storage systems including forecast-based operation strategies. *Appl. Energy* **2018**, *229*, 884–899. [\[CrossRef\]](#)
- Puranen, P.; Kosonen, A.; Ahola, J. Techno-economic viability of energy storage concepts combined with a residential solar photovoltaic system: A case study from Finland. *Appl. Energy* **2021**, *298*, 117199. [\[CrossRef\]](#)
- Parra, D.; Patel, M.K. Effect of tariffs on the performance and economic benefits of PV-coupled battery systems. *Appl. Energy* **2016**, *164*, 175–187. [\[CrossRef\]](#)
- Zou, B.; Peng, J.; Li, S.; Li, Y.; Yan, J.; Yang, H. Comparative study of the dynamic programming-based and rule-based operation strategies for grid-connected PV-battery systems of office buildings. *Appl. Energy* **2022**, *305*, 117875. [\[CrossRef\]](#)
- Wang, G.; Zhang, Q.; Li, H.; McLellan, B.C.; Chen, S.; Li, Y.; Tian, Y. Study on the promotion impact of demand response on distributed PV penetration by using non-cooperative game theoretical analysis. *Appl. Energy* **2017**, *185*, 1869–1878. [\[CrossRef\]](#)
- Sivaneasan, B.; Kandasamy, N.K.; Lim, M.L.; Goh, K.P. A new demand response algorithm for solar PV intermittency management. *Appl. Energy* **2018**, *218*, 36–45. [\[CrossRef\]](#)
- Nyholm, E.; Odenberger, M.; Johnsson, F. An economic assessment of distributed solar PV generation in Sweden from a consumer perspective—The impact of demand response. *Renew. Energy* **2017**, *108*, 169–178. [\[CrossRef\]](#)
- Zhao, J.; Kucuksari, S.; Mazhari, E.; Son, Y.-J. Integrated analysis of high-penetration PV and PHEV with energy storage and demand response. *Appl. Energy* **2013**, *112*, 35–51. [\[CrossRef\]](#)
- Liu, Z.; Zhao, Y.; Wang, X. Long-term economic planning of combined cooling heating and power systems considering energy storage and demand response. *Appl. Energy* **2020**, *279*, 115819. [\[CrossRef\]](#)
- Lorenzi, G.; Silva, C.A.S. Comparing demand response and battery storage to optimize self-consumption in PV systems. *Appl. Energy* **2016**, *180*, 524–535. [\[CrossRef\]](#)
- Bashir, A.A.; Kasmaei, M.P.; Safdarian, A.; Lehtonen, M. Matching of Local Load with On-Site PV Production in a Grid-Connected Residential Building. *Energies* **2018**, *11*, 2409. [\[CrossRef\]](#)



19. Salpakari, J.; Rasku, T.; Lindgren, J.; Lund, P.D. Flexibility of electric vehicles and space heating in net zero energy houses: An optimal control model with thermal dynamics and battery degradation. *Appl. Energy* **2017**, *190*, 800–812. [[CrossRef](#)]
20. Nyholm, E.; Puranik, S.; Mata, É.; Odenberger, M.; Johnsson, F. Demand response potential of electrical space heating in Swedish single-family dwellings. *Build. Environ.* **2016**, *96*, 270–282. [[CrossRef](#)]
21. Zhang, Z.; Guéguen, H. Bilevel Optimization Based on Building Dynamic Flexibility Capacity in Microgrid. *Ifac-Papersonline* **2022**, *55*, 274–279. [[CrossRef](#)]
22. Chen, Y.; Xu, P.; Chen, Z.; Wang, H.; Sha, H.; Ji, Y.; Zhang, Y.; Dou, Q.; Wang, S. Experimental investigation of demand response potential of buildings: Combined passive thermal mass and active storage. *Appl. Energy* **2020**, *280*, 115956. [[CrossRef](#)]
23. Mauro, A.; Buonomano, A.; Athienitis, A. Design for energy flexibility in smart buildings through solar based and thermal storage systems: Modelling, simulation and control for the system optimization. *Energy* **2022**, *260*, 125024. [[CrossRef](#)]
24. da Fonseca, A.L.; Chvatal, K.M.; Fernandes, R.A. Thermal comfort maintenance in demand response programs: A critical review. *Renew. Sustain. Energy Rev.* **2021**, *141*, 110847. [[CrossRef](#)]
25. Aghniaey, S.; Lawrence, T.M. The impact of increased cooling setpoint temperature during demand response events on occupant thermal comfort in commercial buildings: A review. *Energy Build.* **2018**, *173*, 19–27. [[CrossRef](#)]
26. Finlex, Sänkotoimitusehdot (In Finnish). Available online: <https://www.finlex.fi/fi/laki/alkup/1989/19891179> (accessed on 20 April 2022).
27. Koskela, J.; Rautiainen, A.; Järventausta, P. Utilization Possibilities of Electrical Energy Storages in Households' Energy Management in Finland. *Int. Rev. Electr. Eng.* **2016**, *11*, 607–617. [[CrossRef](#)]
28. Duffie, J.A.; Beckman, W.A. *Solar Engineering of Thermal Processes*, 3rd ed.; John Wiley & Sons, Inc.: Hoboken, NJ, USA, 2006.
29. Vartiainen, E. A new approach to estimating the diffuse irradiance on inclined surfaces. *Renew. Energy* **2000**, *20*, 45–64. [[CrossRef](#)]
30. Perez, R.; Ineichen, P.; Seals, R.; Michalsky, J.; Stewart, R. Modeling daylight availability and irradiance components from direct and global irradiance. *Sol. Energy* **1990**, *44*, 271–289. [[CrossRef](#)]
31. Reindl, D.T.; Beckman, W.A.; Duffie, J.A. Diffuse fraction correlations. *Sol. Energy* **1990**, *45*, 1–7. [[CrossRef](#)]
32. Padovan, A.; Del Col, D. Measurement and modeling of solar irradiance components on horizontal and tilted planes. *Sol. Energy* **2010**, *84*, 2068–2084. [[CrossRef](#)]
33. Hellman, H.-P.; Koivisto, M.; Lehtonen, M. Photovoltaic power generation hourly modelling. In Proceedings of the International Scientific Conference on Electric Power Engineering, Brno, Czech Republic, 12–14 May 2014; pp. 269–272. [[CrossRef](#)]
34. Nykvist, B.; Nilsson, M. Rapidly falling costs of battery packs for electric vehicles. *Nat. Clim. Chang.* **2015**, *5*, 329–332. [[CrossRef](#)]
35. Fernão Pires, V.; Romero-Cadaval, E.; Vinnikov, D.; Roasto, I.; Martins, J.F. Power converter interfaces for electrochemical energy storage systems—A review. *Energy Convers. Manag.* **2014**, *86*, 453–475. [[CrossRef](#)]
36. Tremblay, O.; Dessaint, L.-A.; Dekkiche, A.-I. A Generic Battery Model for the Dynamic Simulation of Hybrid Electric Vehicles. In Proceedings of the IEEE Vehicle Power and Propulsion Conference, Arlington, TX, USA, 9–12 September 2007; pp. 284–289.
37. Mehrbankhomartash, M.; Rayati, M.; Sheikhi, A.; Ranjbar, A.M. Practical battery size optimization of a PV system by considering individual customer damage function. *Renew. Sustain. Energy Rev.* **2017**, *67*, 36–50. [[CrossRef](#)]
38. Hietaharju, P.; Ruusunen, M.; Leiviskä, K. A Dynamic Model for Indoor Temperature Prediction in Buildings. *Energies* **2018**, *11*, 1477. [[CrossRef](#)]
39. Mutanen, A.; Ruska, M.; Repo, S.; Jarventausta, P. Customer Classification and Load Profiling Method for Distribution Systems. *IEEE Trans. Power Deliv.* **2011**, *26*, 1755–1763. [[CrossRef](#)]
40. Finnish Meteorological Institute, Open Data. Available online: <https://en.ilmatieteenlaitos.fi/open-data> (accessed on 7 April 2022).
41. Koskela, J.; Mutanen, A.; Järventausta, P. Using Load Forecasting to Control Domestic Battery Energy Storage Systems. *Energies* **2020**, *13*, 3946. [[CrossRef](#)]
42. Statistics Finland, Number of Buildings by Heating Fuel 1970–2020. Available online: [https://www.stat.fi/til/rakke/2020/rakke\\_2020\\_2021-05-27\\_tau\\_002\\_en.html](https://www.stat.fi/til/rakke/2020/rakke_2020_2021-05-27_tau_002_en.html) (accessed on 7 April 2022).

**Disclaimer/Publisher's Note:** The statements, opinions and data contained in all publications are solely those of the individual author(s) and contributor(s) and not of MDPI and/or the editor(s). MDPI and/or the editor(s) disclaim responsibility for any injury to people or property resulting from any ideas, methods, instructions or products referred to in the content.